

A structure-based approach towards identification of inhibitory fragments for eleven-nineteen-leukemia protein (ENL) YEATS domain

David Heidenreich^{1,3}, Moses Moustakim^{2,4}, Jurema Schmidt¹, Daniel Merk¹, Paul E. Brennan², Oleg Fedorov², Apirat Chaikuad^{1,3*}, Stefan Knapp^{1,3*}

¹ Institute of Pharmaceutical Chemistry, Goethe-University Frankfurt, 60438 Frankfurt, Germany

² Target Discovery Institute and Structural Genomics Consortium, University of Oxford, Oxford OX3 7DQ, UK

³ Structural Genomics Consortium, BMLS, Goethe-University Frankfurt, 60438 Frankfurt, Germany

⁴ Department of Chemistry, University of Oxford, Chemistry Research Laboratory, Oxford, OX1 3TA, UK

ABSTRACT: Lysine acetylation is an epigenetic mark that is principally recognized by bromodomains and recently structurally diverse YEATS domains also emerged as readers of lysine acetyl/acylations. Here we present a crystallography-based strategy and the discovery of fragments binding to the ENL YEATS domain, a potential drug target. Crystal structures combined with synthetic efforts led to the identification of a sub-micromolar binder, providing first starting points for the development of chemical probes for this reader domain family.

Post-translation modification at lysines is one of the key mechanisms that regulates epigenetic signaling. Lysine acetylation (Kac) is one of the most common epigenetic “marks”, which is specifically recognized by bromodomains and some double PHD finger (DPF) domains¹⁻². Recently, YEATS domains emerged as a third class of histone acetylation readers which are present in four human proteins: ENL (MLLT1), YEATS2, AF9 (MLLT3) and glioma amplified sequence 41 (GAS41 or YEATS4). Interaction with acetylated histones was first demonstrated for AF9³ and subsequently also confirmed for the remaining family members⁴⁻⁶. Interestingly, YEATS domains display an expanded reader activity, also recognizing other types of lysine modifications including propionylation, butyrylation and crotonylation^{3, 7-9}.

The YEATS domain constitutes ~120-140 amino acids and is evolutionarily conserved from yeast to human¹⁰. It exhibits an immunoglobulin-like topology with an elongated β -sheet sandwich core capped by one or two short helices^{3, 11}. The binding pocket is constructed by three loops emanating from the Ig fold. A number of conserved aromatic residues shape a flat, extended architecture of the binding groove, that is capable of recognizing acyl-lysine containing sequences^{3-7, 9}. The proteins harboring the YEATS reader domain are often associated with histone acetyl transferase (HAT) and chromatin-remodeling complexes¹²⁻¹³, implicating their diverse roles in the regulation of chromatin structure, histone acetylation, gene transcription, stress signaling, mitotic progression and DNA damage response^{3, 13-15}. In addition, the ability to preferentially recognize other lysine acylation marks suggests that the YEATS family proteins might exert differential regulatory functions than the prototypical Kac reader families with their own cognate targets¹⁶.

Dysfunction of YEATS proteins has been linked to diseases, notably cancer. For instance, the fusion of AF9 or ENL and human mixed lineage leukemia (MLL) proteins are frequently

found in acute myeloid leukemia, and these fusions constitute oncogenes that are drivers of this highly aggressive cancer^{5, 17-18}. In addition, GAS41, a common subunit of SRCAP (Snf2 related CREBBP activator protein) and Tip60 HAT complexes, is a growth-promoting protein^{12, 19}. These roles suggest that YEATS proteins are potential targets for drug development. Indeed, two recent studies identified the ENL (MLLT1) YEATS domain as a compelling target in AML^{5, 17}.

Development of chemical probes targeting the acetyl-lysine readers, the bromodomain family, provided significant insight into the biological function of these proteins and their potential as drug targets²⁰⁻²². However, in contrast to bromodomains, no inhibitors of YEATS have been reported to date. This prompted us to identify chemical scaffolds that can interact with the binding pocket of this acetyl-lysine reader family, focusing on oncogenic ENL. In a similar manner to bromodomains, we chose a structure-based approach to identify initial fragment binders²³⁻²⁶. We predicted an essential chemical moiety that could mimic β -sheet type hydrogen bonding pattern of acylated lysine, and established a small fragment-like library. Using structure-based approaches as well as biophysical characterization such as thermal shift and isothermal calorimetry (ITC), we identified potential inhibitory ligands for ENL, which may provide chemical starting points for further development of potent inhibitors for this protein as well as the other members of the histone acylation reader YEATS family.

To date all available crystal structures of ENL and other YEATS proteins have been solved in complexes with peptides. We therefore determined the apo-structure of ENL to expand our knowledge on a non-liganded form of the protein. In the ENL apo-structure, all structural elements were well defined by electron density, including loop 1 (L1), 4 (L4) and 6 (L6) that defined the recognition site for acylated lysine (Figure 1A and Supplementary Figure S1). This suggested that the binding pocket is well-structured prior to the binding of the ligands.

Nonetheless, surprisingly, the side chain of Y78 located on L6, which is together with F28 and F59 part of the conserved aromatic acyl-lysine binding triad, exhibited two orientations not observed previously in the peptide-complexed structures. The ‘in’ conformation with the side chain positioned on top of the binding site resembled the orientation observed in ENL-K_{ac}27H3 complex, while the ‘out’ conformation exhibited a 90° side chain rotation. This conformation was stabilized by a hydrogen bond to the backbone of L1 E26. The unexpected flexibility of this tyrosine suggested therefore an intrinsic flexible nature of the binding site, interchangeable between the confined ‘in’ conformation and a more open surface when adopting the ‘out’ conformation.

Despite sharing acetyl-lysine recognition functions, comparative analyses revealed diverse features between canonical acetyl-lysine binding sites of ENL and bromodomains such as BRD4² (Figure 1A and 1B). First, the two families harbored distinct primary, secondary and tertiary structure and therefore have diverse acetyl-lysine binding sites. In bromodomains, the acetyl moiety is anchored by hydrogen bonds to a conserved asparagine and via a water to a tyrosine residue (N140 and Y97 in BRD4)^{2, 27}. In contrast, in ENL the backbone of loop 6 and the aromatic triad (F28, F59 and Y97 in ENL) mediate this recognition process^{3, 5}. In addition, the two readers exploited different structural elements towards a formation of the pocket. Two helices and the ZA loop, acting as a selectivity filter for both protein partners and small molecule inhibitors, contributed to a deep, groove-like construction in bromodomains², which was in contrast to a surface-exposed, tunnel-like pocket formed through three loop elements and the side chains of the aromatic triad in ENL (Figure 1C and 1D). These differences resulted also in diverse patterns of conserved water molecules present in the pockets. Typically five water molecules conducting a complex hydrogen bond network in bromodomains²⁸⁻²⁹ compared to two structural waters present in ENL located adjacent to Y78 and A79 backbones (Figure 1).

Comprehensive structural analyses revealed that the distinct cave-like characteristic of the pocket in ENL, as well as in other YEATS members, may well be evolved for its compatibility with various lysine acylation. The front open adjacent to H56 and loop6 A79 provides a more restrained entrance for lysine backbone, while the rear open end cradled by F28 and F59 adopts a flat, hydrophobic environment for accepting the elongated acylation modification such as K_{cr}^{7, 9} (Figure 3A). The profound structural differences between the pockets of bromodomains and YEATS domains therefore suggested that current acetyl-lysine mimetic bromodomain ligands are unlikely to bind to YEATS domains. With a largely hydrophobic and aromatic surface area of ~93 Å² and a pocket volume of ~34 Å³, the ENL binding pocket is smaller than most bromodomain binding sites, yet could be sufficiently large for the development of potent inhibitors.

The unique features of the ENL pocket prompted us to presume that the narrow binding site with two open ends might be able to accommodate linear molecules harboring a central carbonyl group, which were considered as initial fragment-like scaffolds (Figure 3A). For fragment selection, we postulated that suitable ligands should contain i) a central amide functional group to mimic acetyl-lysine and ii) at least an aromatic property at carbonyl (R¹) end or, if flipped amide, nitrogen (R²) end to mimic μ -stacking with F28 and F59, an interaction observed for the crotonyl group (K_{cr}) (Figure 3B).

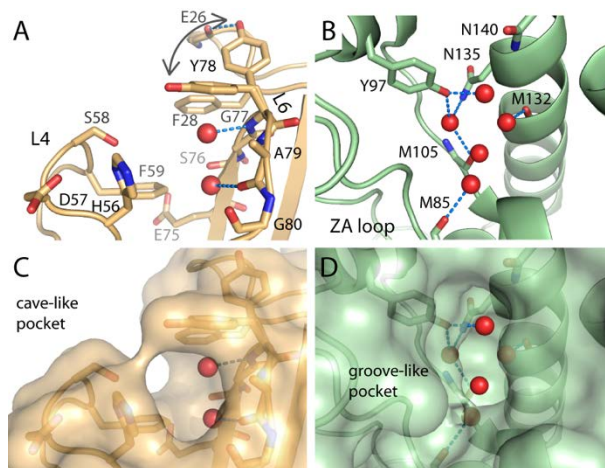


FIGURE 1 Structure of apo-ENL (pdb code, 6hq0). A) close-up details of the binding site of ligand-free ENL with Y78, a residue part of the key interacting aromatic triad, adopting two flexible conformations. Bound water molecules within the pocket are shown in red spheres. B) acetyl-lysine binding pocket of BRD4 (pdb id: 2OSS) with conserved asparagine (N140), tyrosine residue (Y97) and water network (red spheres) displayed. Surface representation of the binding sites of ENL (C) and BRD4 (D) reveals distinct pocket shapes between these two acetyl-lysine binding reader families.

Based on this assumption, we first selected a small set of 19 fragment-like compounds, which were classified into four groups based on the positions of their aromatic rings; i) only on R² (1-7), ii) only on R¹ (8), iii) on both R¹ and R² (9-14), iv) on R² with a spacing atom prior to attachment on R¹ (15-18), and v) on R¹ with a spacing atom prior to attachment on R² (19) (Figure 3C and Supplementary Figure S2). These compounds were initially tested using thermal shift assays, unfortunately no detectable shifts in melting temperature were observed (data not shown). We then sought to exploit an alternative crystallography-based approach, to verify interaction and to determine binding modes. Ligand soaking was performed for all compounds, however only 10 crystals with 1, 2, 3, 9, 10, 11, 12, 14, 15 and 19 still preserved diffraction quality. Examination of electron density maps revealed in all structures additional density in proximity to Y78 backbone where the carbonyl of bound acetyl-lysine was typically situated (Figure 3 and Supplementary Figure S3). This consistent observation likely confirmed our hypotheses of the use of a central amide group as an acetyl-lysine mimetic for ENL. However, an assessment of the ligand binding modes was only possible for compound 12 and 19, where a complete trace of electron density enabled an accurate placement of the ligands (Figure 3D). These compounds were from two different groups in our selection yet their binding modes were similar. First, the amide core was observed to flip in comparison to that of acetyl-lysine. While the carbonyl of the flipped amide maintained the β -sheet type hydrogen bonding pattern of acylated lysine to Y78 backbone, the nitrogen group further engaged a direct bond to the S58 side chain that swung slightly backwards. At the front end of the ENL pocket both aromatic benzene and benzimidazole groups of 12 and 19, respectively, attached to the amide carbonyl at R¹ were sandwiched between loop4 H56 and loop 6 A79, adopting a nearly planar orientation to the histidine imidazole. The decorations of the R¹ aromatic groups of both compounds were highly solvent exposed, showing little or no interaction to the protein.

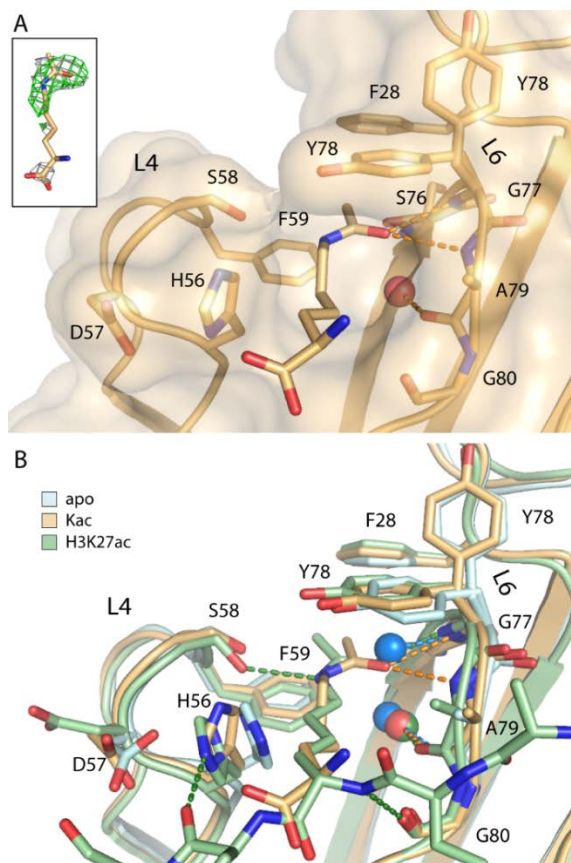


FIGURE 2 Structure of ENL in complex with acetyl-lysine. A) Detailed interaction between the bound Kac within ENL (pdb code, 6hpz). Inset shows $|F_o| - |F_c|$ omitted electron density map contoured at 3σ (green) and $|2F_o| - |F_c|$ refined map contoured at 1σ (grey) for the bound ligand. B) Superimposition of apo, Kac-bound, and H3K27ac-complexed (pdb id: 5J9S) ENL structures revealed a conserved binding mode of Kac that displaced a water for a hydrogen bond interacting with the Y78 backbone amine. The presence of the ligand or peptide induced structural alterations at Y78, H56 and D57.

Surprisingly, accommodation of the R^2 decoration at the rear pocket were highly different between these two ligands. For **12**, the R^2 benzene ring directly attached on to the amide nitrogen atom tucked in planar in between F28 and F59, and potentially formed three-layer μ -stacking with these phenylalanine residues, an interaction expected to mimic lysine crotonylation. In contrast, a similar interaction was not observed for the chlorobenzene of **19**. This could be due to a constraint geometry of the sp^3 carbon spacing atom at R^2 , which in comparison to **12** forced a rotation of nearly 120° to ascend the chlorobenzene group outwards from the rear pocket to the solvent exposed region. The orientation of the ring system of **19** potentially also created steric constraints for Y78, and consequently induced the tyrosine to adopt the ‘out’ conformation. Unlike **12**, this conformation of Y78 resulted in a rather exposed, less rigid pocket. Both co-crystal structures of ENL with **12** and **19** provided valuable structural insights into the binding mode highlighting for example the importance of direct attachments of the aromatic moieties to the R^1 and R^2 position of the amide core, which may provide fundamental keys not only for a decrease of flexibility of both ligands and Y78 but for enhancing optimal conditions for strong π - π contacts. In parallel, development of a high-

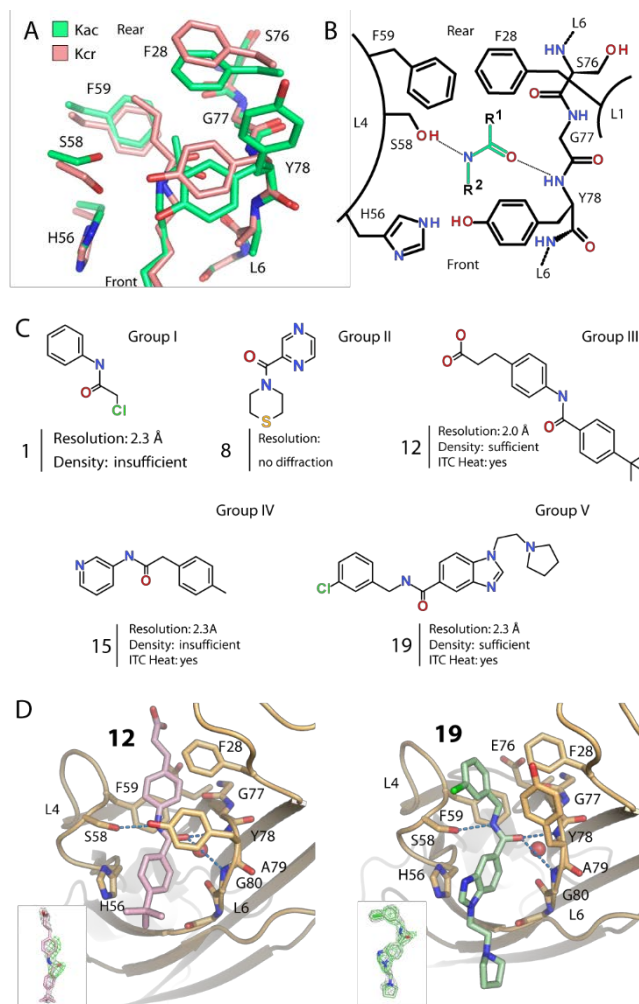


FIGURE 3 Crystallography-based screening approach. A) Analyses of the binding pockets of ENL and YEATS family reveals an open binding site. B) Schematic illustration of key residues within the pocket and the design of acetyl-lysine mimetics containing an amide core mimicking a β -sheet hydrogen bond interaction and an aromatic decoration at R^1 or R^2 for π - π interactions with F28 and F59. C) Examples of selected ligands. D) Structures of ENL in complex with **12** (top, pdb code, 6hpy) and **19** (bottom, pdb code, 6hpx). Insets show $|F_o| - |F_c|$ omitted and $|2F_o| - |F_c|$ electron density map contoured at 3σ (green) and 1σ (grey), respectively. Hydrogen bonds are shown as dashed lines and water molecules as red spheres.

throughput assay and screening identified similar chemotypes, in essence a benzimidazole-amide hit with low micromolar affinity³⁰.

To test this chemical scaffold, we used our available chemistry to preliminarily synthesize a small set of R^2 -benzimidazole amide derivatives with modification on R^1 , resulting in compounds **20–24** (Figure 4A). Using ITC, we observed that these derivatives bound ENL with good affinities in low micromolar range with compound **20** showing the best potency demonstrating a submicromolar K_d of $0.8 \mu\text{M}$. We then focused on characterizing of the binding mode of **20**, and successful soaking and structure determination enabled an insight into the binding mode of this compound in ENL. As expected the Kac mimetic amide core retained its flipped binding orientation maintaining the interactions to Y78 and S58 as observed for **12** and **19** (Figure 4B). The R^1 3-iodo-4-methylbenzene was situated in the

front cavity, adopting a planar conformation to H56 for a π -stacking contact (distance ~ 4 Å). The R² benzimidazole as expected located at the rear pocket was sandwiched between and feasibly induced a three-layer π -stacking with F28 and F59. However, apart from these predictable fundamental key interactions compound **20** was observed to engage further hydrogen bonds to the protein, which were not present previously in **12** and **19**. This included a direct contact between the nitrogen of the benzimidazole ring and S76 backbone carbonyl. In addition, the extended piperidine decoration was observed to protrude further along the protein surface at the rear end, where it exerted a conformation that enabled a direct contact between its nitrogen with the E75 carboxylic side chain (distance of ~ 3.1 Å). We performed ITC to assess thermodynamics of the binding of **12**, **19** and **20** to ENL (Figure 4C). Binding of **20** was characterized by a favorable enthalpic binding enthalpy and a K_d of ~ 807 nM. Binding enthalpy was observed for **12** and **19** indicating interactions in the 20–50 μ M K_d region. The presented data demonstrate that the acetyl-lysine binding site of ENL is druggable using a central aromatic scaffold decorated with an amide that acts as acetyl-lysine mimetic moiety.

YEATS domains have a fundamentally different binding site than the well-explored acetyl-lysine readers of the bromodomain family. These differences enable YEATS domains to also recognize larger modifications at the ϵ -nitrogen of lysines including crotonylation and others acyl-modifications not recognized by bromodomains which typically have a closed water-filled binding pocket. Thus, targeting YEATS domains will require a different design of acyl-lysine mimetic inhibitors. The information provided by this structure-based fragment study will facilitate this design and the development of more potent inhibitors. In our laboratory, we used benzimidazole amides for the development of a potent chemical probe for ENL and AF9³¹, which will facilitate further study of the role of this interesting reader domain in normal physiology and disease.

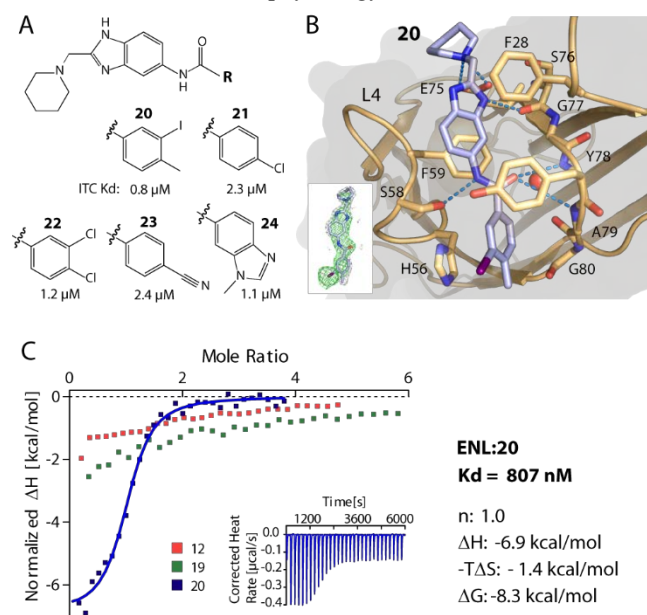


Figure 4 Benzimidazole-amide derivatives and characterization of the interaction of **20** with ENL. A) Chemical structures of a set of benzimidazole-amide derivatives and their ITC K_d values. B) Crystal structure of the ENL complex with **20** (pdb code, 6hpw). Insets show $|F_o| - |F_c|$ omitted electron density map contoured at 3σ (green) and $|2F_o| - |F_c|$ refined map contoured at 1σ (grey). C)

ITC normalized binding heat of the interactions between **12**, **19** and **20** with ENL. Inset shows the isotherm of raw injection heats for **20**.

EXPERIMENTAL SECTION

Protein purification, crystallization and structure determination - ENL YEATS domain (1–148) was sub-cloned into pNIC-CH, and the recombinant protein incorporating a non-cleavable C-terminal His₆-tag was expressed *E. coli* Rosetta. Purification was performed using Ni²⁺ affinity and size-exclusion chromatography. Pure protein in 25 mM Tris pH 7.5, 300 mM NaCl, 0.2 mM TCEP was concentrated to 0.45 mM, and was used for crystallization at 20 °C and various reservoir solutions using PEG/PEG smears³² as precipitant (Supplementary table S1). Ligands at 5–40 mM concentration were soaked into crystals, which were subsequently cryo-protect with 25% ethylene glycol. Diffraction data collected at BESSY II, SLS, and Diamond Light Source were processed using XDS³³ or iMOSFLM³⁴ and scaled with aimless³⁵. Molecular replacement was performed in PHASER³⁶ using pdb-id: 5J9s. Model rebuilding alternated with structure refinement was performed in COOT³⁷ and REFMAC³⁸. The models were verified using molprobity³⁹. Data collection and refinement statistics are summarized in Suppl. table S1.

Compounds used in this study were obtained from commercial source (ChemDiv (1–7, 9–10, 13–15, 17–19), Enamine (8 and 16)), except **11**, **12**, **20–24**, which were synthesized and checked for their purity of $>95\%$ using either the stated Waters UHPLC or the Varian ProStar HPLC. Detailed syntheses and characterizations are provided in Supplementary information.

Isothermal titration calorimetry data were measured with a NanoITC instrument (TA instruments) at 25°C. Protein at 300 μ M in 25 mM Tris pH 7.5, 500 mM NaCl, 0.5 TCEP, 5% glycerol was titrated into 20–30 μ M compounds.

ASSOCIATED CONTENT

Supporting Information. The Supporting Information is available free of charge at <http://pubs.acs.org>.

AUTHOR INFORMATION

Corresponding Authors: knapp@pharmchem.uni-frankfurt.de; chaikuad@pharmchem.uni-frankfurt.de.

Author Contributions

AC and SK wrote the paper with contributions of all authors. DH conducted the experiments, MM, DM and JS contributed inhibitors, PB, OF, SK, AC supervised research. All authors have given approval to the final version of the manuscript.

Notes

Coordinates and structure factors have been deposited: accession codes 6hq0, 6hpw, 6hpx, 6hpy and 6hpz.

ACKNOWLEDGMENT

The SGC, a registered charity that receives funds from AbbVie, Bayer Pharma AG, Boehringer Ingelheim, Canada Foundation for Innovation, Eshelman Institute for Innovation, Genome Canada, Innovative Medicines Initiative [ULTRA-DD 115766], Wellcome Trust, Janssen, Merck & Co., Novartis Pharma AG, Ontario Ministry of Economic Development and Innovation, Pfizer, São Paulo Research Foundation-FAPESP, Takeda and the Centre of Excellence Macromolecular complexes (CEF). S.K. and A.C. are supported by the Sonderforschungsbereich SFB1177 Autophagy.

M.M. is grateful to the EPSRC Centre for Doctoral Training in Synthesis for Biology and Medicine (EP/L015838/1) for a studentship, supported by AstraZeneca, Diamond, Defence Science and Technology Laboratory, Evotec, GlaxoSmithKline, Janssen, Novartis, Pfizer, Syngenta, Takeda, UCB and Vertex. The authors thank staffs at BESSY II, SLS and Diamond Light Source for their support.

ABBREVIATIONS

YEATS domain, The Yaf9, ENL, AF9, Taf14, Sas5 (YEATS) domain; ENL, eleven-nineteen-leukemia protein; MLLT1, myeloid/lymphoid or mixed-lineage leukemia translocated to, chromosome 1 protein; AF9, ALL1-fused gene from chromosome 9 protein; MLLT3, myeloid/lymphoid or mixed-lineage leukemia translocated to chromosome 3 protein.

REFERENCES

- Dhalluin, C.; Carlson, J. E.; Zeng, L.; He, C.; Aggarwal, A. K.; Zhou, M. M., Structure and ligand of a histone acetyltransferase bromodomain. *Nature* **1999**, *399* (6735), 491-496.
- Filippakopoulos, P.; Picaud, S.; Mangos, M.; Keates, T.; Lambert, J. P.; Barsyte-Lovejoy, D.; Felletar, I.; Volkmer, R.; Muller, S.; Pawson, T.; Gingras, A. C.; Arrowsmith, C. H.; Knapp, S., Histone recognition and large-scale structural analysis of the human bromodomain family. *Cell* **2012**, *149* (1), 214-231.
- Li, Y.; Wen, H.; Xi, Y.; Tanaka, K.; Wang, H.; Peng, D.; Ren, Y.; Jin, Q.; Dent, S. Y.; Li, W.; Li, H.; Shi, X., AF9 YEATS domain links histone acetylation to DOTIL-mediated H3K79 methylation. *Cell* **2014**, *159* (3), 558-571.
- Mi, W.; Guan, H.; Lyu, J.; Zhao, D.; Xi, Y.; Jiang, S.; Andrews, F. H.; Wang, X.; Gagea, M.; Wen, H.; Tora, L.; Dent, S. Y. R.; Kutateladze, T. G.; Li, W.; Li, H.; Shi, X., YEATS2 links histone acetylation to tumorigenesis of non-small cell lung cancer. *Nat Commun* **2017**, *8* (1), 1088.
- Wan, L.; Wen, H.; Li, Y.; Lyu, J.; Xi, Y.; Hoshii, T.; Joseph, J. K.; Wang, X.; Loh, Y. E.; Erb, M. A.; Souza, A. L.; Bradner, J. E.; Shen, L.; Li, W.; Li, H.; Allis, C. D.; Armstrong, S. A.; Shi, X., ENL links histone acetylation to oncogenic gene expression in acute myeloid leukaemia. *Nature* **2017**, *543* (7644), 265-269.
- Hsu, C. C.; Zhao, D.; Shi, J.; Peng, D.; Guan, H.; Li, Y.; Huang, Y.; Wen, H.; Li, W.; Li, H.; Shi, X., Gas41 links histone acetylation to H2A.Z deposition and maintenance of embryonic stem cell identity. *Cell Discov* **2018**, *4*, 28, 3-17.
- Li, Y.; Sabari, B. R.; Panchenko, T.; Wen, H.; Zhao, D.; Guan, H.; Wan, L.; Huang, H.; Tang, Z.; Zhao, Y.; Roeder, R. G.; Shi, X.; Allis, C. D.; Li, H., Molecular Coupling of Histone Crotonylation and Active Transcription by AF9 YEATS Domain. *Mol Cell* **2016**, *62* (2), 181-193.
- Andrews, F. H.; Shinsky, S. A.; Shanle, E. K.; Bridgers, J. B.; Gest, A.; Tsun, I. K.; Krajewski, K.; Shi, X.; Strahl, B. D.; Kutateladze, T. G., The Taf14 YEATS domain is a reader of histone crotonylation. *Nat Chem Biol* **2016**, *12* (6), 396-398.
- Zhao, D.; Guan, H.; Zhao, S.; Mi, W.; Wen, H.; Li, Y.; Zhao, Y.; Allis, C. D.; Shi, X.; Li, H., YEATS2 is a selective histone crotonylation reader. *Cell Res* **2016**, *26* (5), 629-632.
- Le Masson, I.; Yu, D. Y.; Jensen, K.; Chevalier, A.; Courbeyrette, R.; Boulard, Y.; Smith, M. M.; Mann, C., Yaf9, a novel NuA4 histone acetyltransferase subunit, is required for the cellular response to spindle stress in yeast. *Mol Cell Biol* **2003**, *23* (17), 6086-6102.
- Wang, A. Y.; Schulze, J. M.; Skordalakes, E.; Gin, J. W.; Berger, J. M.; Rine, J.; Kobor, M. S., Asf1-like structure of the conserved Yaf9 YEATS domain and role in H2A.Z deposition and acetylation. *Proc Natl Acad Sci U S A* **2009**, *106* (51), 21573-21578.
- Schulze, J. M.; Wang, A. Y.; Kobor, M. S., YEATS domain proteins: a diverse family with many links to chromatin modification and transcription. *Biochem Cell Biol* **2009**, *87* (1), 65-75.
- Andrews, F. H.; Shanle, E. K.; Strahl, B. D.; Kutateladze, T. G., The essential role of acetyllysine binding by the YEATS domain in transcriptional regulation. *Transcription* **2016**, *7* (1), 14-20.
- Shanle, E. K.; Andrews, F. H.; Meriesh, H.; McDaniel, S. L.; Dronamraju, R.; DiFiore, J. V.; Jha, D.; Wozniak, G. G.; Bridgers, J. B.; Kerschner, J. L.; Krajewski, K.; Martin, G. M.; Morrison, A. J.; Kutateladze, T. G.; Strahl, B. D., Association of Taf14 with acetylated histone H3 directs gene transcription and the DNA damage response. *Genes Dev* **2015**, *29* (17), 1795-1800.
- Zhao, D.; Li, Y.; Xiong, X.; Chen, Z.; Li, H., YEATS Domain-A Histone Acylation Reader in Health and Disease. *J Mol Biol* **2017**, *429* (13), 1994-2002.
- Dutta, A.; Abmayr, S. M.; Workman, J. L., Diverse Activities of Histone Acylations Connect Metabolism to Chromatin Function. *Mol Cell* **2016**, *63* (4), 547-552.
- Erb, M. A.; Scott, T. G.; Li, B. E.; Xie, H.; Paulk, J.; Seo, H. S.; Souza, A.; Roberts, J. M.; Dastjerdi, S.; Buckley, D. L.; Sanjana, N. E.; Shalem, O.; Nabat, B.; Zeid, R.; Offei-Addo, N. K.; Dhe-Paganon, S.; Zhang, F.; Orkin, S. H.; Winter, G. E.; Bradner, J. E., Transcription control by the ENL YEATS domain in acute leukaemia. *Nature* **2017**, *543* (7644), 270-274.
- Zeisig, D. T.; Bittner, C. B.; Zeisig, B. B.; Garcia-Cuellar, M. P.; Hess, J. L.; Slany, R. K., The eleven-nineteen-leukemia protein ENL connects nuclear MLL fusion partners with chromatin. *Oncogene* **2005**, *24* (35), 5525-5532.
- Heisel, S.; Habel, N. C.; Schuetz, N.; Ruggieri, A.; Meese, E., The YEATS family member GAS41 interacts with the general transcription factor TFIIF. *BMC Mol Biol* **2010**, *11*, 53.
- Filippakopoulos, P.; Knapp, S., Targeting bromodomains: epigenetic readers of lysine acetylation. *Nat Rev Drug Discov* **2014**, *13* (5), 337-356.
- Hewings, D. S.; Rooney, T. P.; Jennings, L. E.; Hay, D. A.; Schofield, C. J.; Brennan, P. E.; Knapp, S.; Conway, S. J., Progress in the development and application of small molecule inhibitors of bromodomain-acetyl-lysine interactions. *J Med Chem* **2012**, *55* (22), 9393-9413.
- Filippakopoulos, P.; Qi, J.; Picaud, S.; Shen, Y.; Smith, W. B.; Fedorov, O.; Morse, E. M.; Keates, T.; Hickman, T. T.; Felletar, I.; Philpott, M.; Munro, S.; McKeown, M. R.; Wang, Y.; Christie, A. L.; West, N.; Cameron, M. J.; Schwartz, B.; Heightman, T. D.; La Thangue, N.; French, C. A.; Wiest, O.; Kung, A. L.; Knapp, S.; Bradner, J. E., Selective inhibition of BET bromodomains. *Nature* **2010**, *468* (7327), 1067-1073.
- Vidler, L. R.; Brown, N.; Knapp, S.; Hoelder, S., Druggability analysis and structural classification of bromodomain acetyl-lysine binding sites. *J Med Chem* **2012**, *55* (17), 7346-7359.
- Ferguson, F. M.; Fedorov, O.; Chaikuad, A.; Philpott, M.; Muniz, J. R.; Felletar, I.; von Delft, F.; Heightman, T.; Knapp, S.; Abell, C.; Ciulli, A., Targeting low-druggability bromodomains: fragment based screening and inhibitor design against the BAZ2B bromodomain. *J Med Chem* **2013**, *56* (24), 10183-10187.
- Chaikuad, A.; Lang, S.; Brennan, P. E.; Temperini, C.; Fedorov, O.; Hollander, J.; Nachane, R.; Abell, C.; Muller, S.; Siegal, G.; Knapp, S., Structure-Based Identification of Inhibitory Fragments Targeting the p300/CBP-Associated Factor Bromodomain. *J Med Chem* **2016**, *59* (4), 1648-1653.
- Chaikuad, A.; Petros, A. M.; Fedorov, O.; Xu, J.; Knapp, S., Structure-based approaches towards identification of fragments for the low-druggability ATAD2 bromodomain. *Medchemcomm* **2014**, *5* (12), 1843-1848.
- Filippakopoulos, P.; Knapp, S., The bromodomain interaction module. *FEBS Lett* **2012**, *586* (17), 2692-2704.
- Aldeghi, M.; Ross, G. A.; Bodkin, M. J.; Essex, J. W.; Knapp, S.; Biggin, P. C., Large-scale analysis of water stability in bromodomain binding pockets with grand canonical Monte Carlo. *Commun Chem* **2018**, *1*-24.
- Aldeghi, M.; Bodkin, M. J.; Knapp, S.; Biggin, P. C., Statistical Analysis on the Performance of Molecular Mechanics Poisson-Boltzmann Surface Area versus Absolute Binding Free Energy Calculations: Bromodomains as a Case Study. *J Chem Inf Model* **2017**, *57* (9), 2203-2221.
- Christott, T.; Bennett, J.; Coxon, C.; Monteiro, O.; Giroud, C.; Beke, V.; Felce, S. L.; Gamble, V.; Gileadi, C.; Poda, G.; Al-Awar, R.; Farnie, G.; Fedorov, O., Discovery of a Selective Inhibitor for the YEATS Domains of ENL/AF9. *SLAS Discov* **2018**, *24* 2555218809904.
- Moustakim, M.; Christott, T.; Monteiro, O. P.; Bennett, J.; Giroud, C.; Ward, J.; Rogers, C. M.; Smith, P.; Panagakou, I.; Saez, L. D.; Felce, S. L.; Gamble, V.; Gileadi, C.; Halidi, N.; Heidenreich, D.; Chaikuad, A.; Knapp, S.; Huber, K. V. M.; Farnie, G.; Heer, J.; Manevski, N.; Poda, G.; Al-Awar, R.; Dixon, D. J.; Fedorov, O.; Brennan, P.,

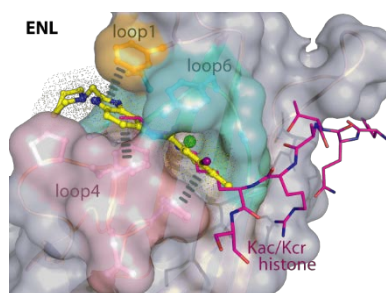
Discovery of an MLLT1/3 YEATS Domain Chemical Probe. *Angew Chem Int Ed Engl* **2018**. [Epub ahead of print]

32. Chaikuad, A.; Knapp, S.; von Delft, F., Defined PEG smears as an alternative approach to enhance the search for crystallization conditions and crystal-quality improvement in reduced screens. *Acta Crystallogr D Biol Crystallogr* **2015**, *71* (Pt 8), 1627-1639.
33. Kabsch, W., Xds. *Acta Crystallogr D Biol Crystallogr* **2010**, *66* (Pt 2), 125-132.
34. Powell, H. R.; Battye, T. G. G.; Kontogiannis, L.; Johnson, O.; Leslie, A. G. W., Integrating macromolecular X-ray diffraction data with the graphical user interface iMosflm. *Nat Protoc* **2017**, *12* (7), 1310-1325.
35. Potterton, L.; Agirre, J.; Ballard, C.; Cowtan, K.; Dodson, E.; Evans, P. R.; Jenkins, H. T.; Keegan, R.; Krissinel, E.; Stevenson, K.; Lebedev, A.; McNicholas, S. J.; Nicholls, R. A.; Noble, M.; Pannu, N. S.; Roth, C.; Sheldrick, G.; Skubak, P.; Turkenburg, J.; Uski, V.; von Delft, F.; Waterman, D.; Wilson, K.; Winn, M.; Wojdyr, M., CCP4i2: the new

graphical user interface to the CCP4 program suite. *Acta Crystallogr D Struct Biol* **2018**, *74* (Pt 2), 68-84.

36. McCoy, A. J., Acknowledging Errors: Advanced Molecular Replacement with Phaser. *Methods Mol Biol* **2017**, *1607*, 421-453.
37. Emsley, P., Tools for ligand validation in Coot. *Acta Crystallogr D Struct Biol* **2017**, *73* (Pt 3), 203-210.
38. Vagin, A. A.; Steiner, R. A.; Lebedev, A. A.; Potterton, L.; McNicholas, S.; Long, F.; Murshudov, G. N., REFMAC5 dictionary: organization of prior chemical knowledge and guidelines for its use. *Acta Crystallogr D Biol Crystallogr* **2004**, *60* (Pt 12 Pt 1), 2184-2195.
39. Williams, C. J.; Headd, J. J.; Moriarty, N. W.; Prisant, M. G.; Videau, L. L.; Deis, L. N.; Verma, V.; Keedy, D. A.; Hintze, B. J.; Chen, V. B.; Jain, S.; Lewis, S. M.; Arendall, W. B., 3rd; Snoeyink, J.; Adams, P. D.; Lovell, S. C.; Richardson, J. S.; Richardson, D. C., MolProbity: More and better reference data for improved all-atom structure validation. *Protein Sci* **2018**, *27* (1), 293-315.

Table of Contents graphic



Structure-based screening approach and initial hit expansion identified a sub-micromolar chemical starting point for the development of ENL YEATS domain inhibitors.
